

CONTROLLED LANDAU DAMPING OF ION-ACOUSTIC WAVES*

I. Alexeff, W. D. Jones, and D. Montgomery†
 Oak Ridge National Laboratory, Oak Ridge, Tennessee
 (Received 31 March 1967)

We have been able to produce Landau damping of ion-acoustic waves at will without appreciably changing the gross parameters—electron temperature, ion temperature, wave velocity, or wave frequency—of the system.

Although several sets of clear-cut Landau-damping experiments have been made on plasma electron waves,¹ only two sets have been made on ion-acoustic waves.^{2,3} Yet the ion-acoustic waves are perhaps more convenient to use than the electron-plasma waves, since the velocity of the ion-acoustic waves is independent of plasma density.

In previous ion-wave experiments, the plasma was supported by a magnetic field, and waves propagated parallel to the field.² Landau damping was controlled by varying the plasma electron temperature.³ As the temperature increased, the wave velocity became appreciably greater than the thermal velocity of the ions, and Landau damping decreased. Note that both the electron temperature and the wave velocity were varied to change the Landau damping.

In the present experiment no magnetic field is needed. The electron temperature does not vary. The wave velocity is kept constant, and is always much higher than the mean velocity of the heavy, primary ions composing the plasma. Under this condition of operation, Landau damping is neither predicted nor observed. However, a trace of light ions is then added to the plasma. The mean thermal velocity of the light ions is comparable to the ion-wave velocity, and Landau damping is both predicted and observed.

The basic system used is shown in Fig. 1. The plasma is produced by a diffuse electron stream, and has been observed to be remarkably quiescent.^{4,5} The plasma parameters for the case with helium are as follows: $T_e = 1.2$ eV, $T_i = 0.052$ eV, $n_e \approx 5 \times 10^8$ cm⁻³, heavy-ion mass = 131 amu (xenon), light-ion mass = 4 amu (helium), discharge current = 150 mA, applied voltage = 22 V, and observed wave velocity = 7.6×10^4 cm sec⁻¹. The determination of the ion temperature was made by five independent techniques. First, the velocity of the ion-acoustic wave at low electron temperatures

yields the ion temperature.⁶ This measurement yields $T_i = 0.052 \pm 0.011$ eV. Second, the radial drift rate of the plasma as measured by ion waves yields a measure of ion temperature.⁴ Third, the observed gas damping of the ion waves with high gas pressure present yields the ion-atom collision rate, and a measure of the ion temperature. Fourth, a measure of Landau damping as a function of electron temperature yields the ion temperature.⁷ Fifth, a computation of the rate of ion heating by collisions with electrons, in the absence of rf noise, reveals that the ions are lost to the wall before they are heated appreciably. All the above ion-temperature measurements are consistent with $T_i \approx 1/20$ eV. Note that the above measurements only yield T_i for xenon, and we must assume that T_i for helium is the same.

Propagation studies are made by means of sine-wave bursts, as are shown in Fig. 2. By using sine-wave bursts, effects caused by direct electrostatic coupling between the transmitting and receiving electrode are eliminat-

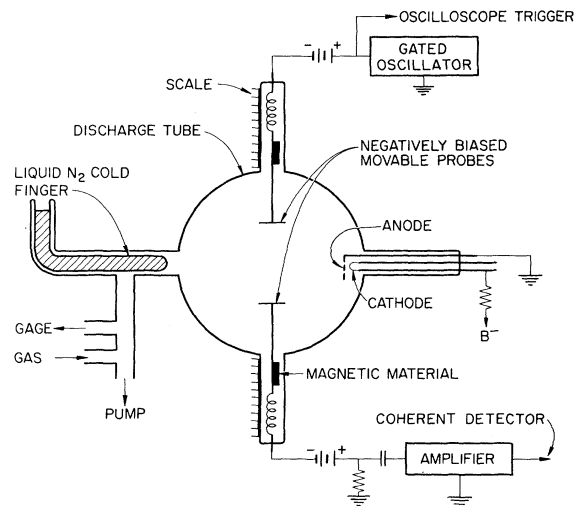


FIG. 1. Schematic of the apparatus used. In this experiment, the spacing of the transmitting and receiving electrodes can be changed by means of a magnet operating on the magnetic material shown. A Langmuir probe (not shown) is used to monitor continuously the plasma electron temperature and density. Both the transmitting and receiving electrodes must be negatively biased.

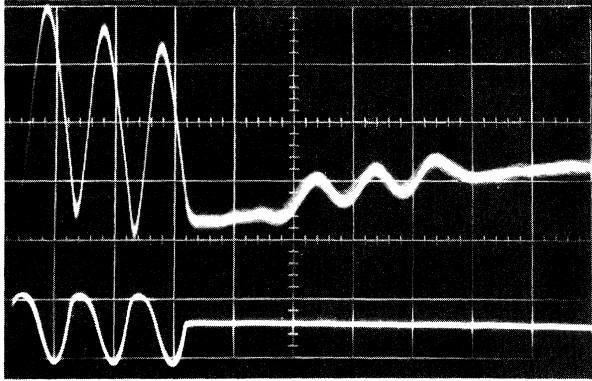


FIG. 2. Typical transmitted and received signals over short distances without using coherent detector. Lower trace, transmitted signal. Upper trace, received signal. Note the strong, directly coupled signal on the receiver trace which is separated from the weaker, ion-wave signal by time of flight. Vertical axis, amplitude (relative units). Horizontal axis, time (10 μsec /large division). The gas used is xenon.

ed. A coherent receiver is used to improve the signal-to-noise ratio. The experimental measurements are made in the center of the spherical vessel, so that wall effects and radial plasma drifts will have little influence on the wave-propagation experiments.

Our Landau-damping measurements are made in the following fashion. With no helium added, the amplitude of the signal is measured as a function of frequency and propagation distance. The signal strength far from the source is observed to decrease as r^{-2} , showing that the voltage output of the receiving probe is proportional to energy. The rate of decrease in amplitude with distance is observed to be frequency independent. Next, helium is added. The amplitude of the received signal now is observed to decrease more rapidly with distance than before. Also, the rate of decrease is observed to be more rapid with increasing frequency. If the plot of received signal versus amplitude is extrapolated back to zero transmission distance, the source strength of the signal is observed not to change appreciably when helium is added. The wave velocity and the electron temperature change only about ten percent. Thus, we assume that the addition of helium does not appreciably perturb the system, other than to provide Landau damping.

The data are analyzed as follows. First,

the observed amplitude of the received signal with helium at each electrode spacing and frequency is divided by the corresponding one without helium. This division, for a given frequency, yields the relative amplitude decrease as a function of distance due to helium alone. Second, the relative decrease of amplitude with distance is fitted by least squares with an exponential function of the form $\exp(-X/X_0)$, where X is the electrode spacing, and X_0 is the observed damping distance for that frequency. Finally, the observed damping distance X_0 is plotted as a function of frequency as shown in Fig. 3.

In Fig. 3, we see that the observed damping distance X_0 varies inversely as the frequency. Thus, the damping cannot be collisional, because for weakly damped waves in free flight, collisional damping is frequency independent. To compare this observed damping with theory, a simple linear approximation, valid for small contamination, and based on the work of Fried and Gould⁸ and Gould,⁹ is used. Here, the spatial damping factor X_0^{-1} is given by

$$X_0^{-1} = \frac{\epsilon \pi^{3/2} (T_e)^{3/2} (m_2)^{1/2}}{\lambda \sqrt{2} (T_i)} \exp\left[-\frac{(m_2 T_e)}{2m_1 T_i}\right],$$

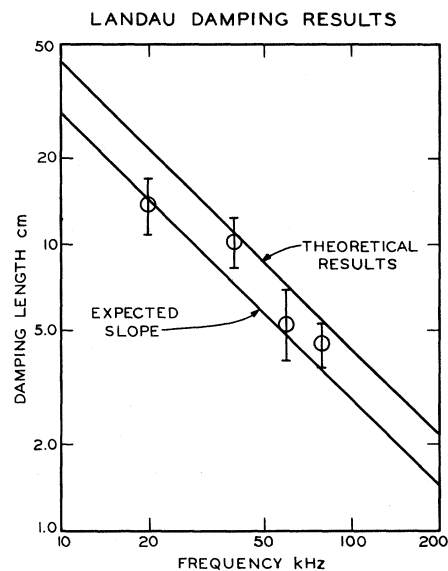


FIG. 3. Experimentally observed and theoretically computed damping distances as a function of frequency. No adjustable parameters are involved in the theoretical calculation. The curve marked "expected slope" corresponds to assuming that $T_i = 1/30$ eV. The curve marked "theoretical results" corresponds to the measured value of $T_i = 0.052$ eV. Data were taken at 20, 40, 60, and 80 kHz.

where ϵ is the ratio of the number density of light to heavy ions, λ is the wavelength of the ion wave, T_e is the electron temperature, T_i is the ion temperature, m_1 is the mass of the heavy ion, and m_2 is the mass of the light ion. As can be seen from this equation, the damping distance X_0 goes directly with wavelength or, for our system which has negligible dispersion, inversely with frequency. Thus, the predicted dependence of damping on frequency is observed.

Landau damping in a one-ion-species plasma shows a strong dependence on the electron-ion temperature ratio. This is due to the strong dependence of the exponential factor in the damping equation on the temperature ratio. In contrast, study of the above equation reveals that for the ion mass and temperature ratios used here, the exponential term is near unity, leading to relatively small changes in the damping rate for small changes in the temperature ratio.

We can also predict quantitatively the expected Landau damping, which is shown by the line marked "theoretical results" in Fig. 3. To accomplish this, the relative fraction of helium ions to xenon ions ϵ in the plasma must be known. We calculate ϵ by first measuring the number of xenon atoms and of helium atoms present in the discharge tube by means of an Alphatron¹⁰ ion gauge. To measure the small amount of helium present, the xenon is turned off at the end of the experiment. Next, the relative ionization cross sections¹¹ of helium and xenon are used to get the relative rates of ion production. For this calculation, we note that the energy of the incoming electrons is cathode plus plasma potential or $22 + 6 = 28$ V. Finally, the ratio of production rates of the two species of ions is weighted by the reciprocal of the ratio of the velocities of escape of the ions to give the relative ion density. Since the ion temperatures are assumed to be equal, the escape velocity is proportional to the reciprocal of the square root of the ion mass. We find that the ratio of the number of helium xenon ions ϵ is about 3.4×10^{-3} . As shown in Fig. 3, this value of ϵ applied to our Landau-damping formula gives a predicted damping that agrees quantitatively within a factor of 2 of the observed value. The computed 20% error in the ratio of T_e/T_i results in a calculated spread for the theoretical X_0^{-1} of less than 25 %.

Experimentally, for a fixed helium contamination, we can change the observed damping distance by varying the frequency over a range of only about 4 to 1. The long damping-distance limit occurs at low frequencies when the wavelength becomes comparable to the dimensions of the apparatus. The short damping-distance limit occurs because the coupling between the transmitting and receiving probes and the plasma is observed to decrease greatly at high frequencies. Even coherent detection,¹² which was used for most of the measurements, was not capable of recovering the damped ion-acoustic wave signals above the frequencies shown. The damping distance has been varied over a wide range, however, by varying the helium concentration.

A third support for assuming that the observed damping is due to Landau damping is obtained from earlier, preliminary experiments done with pulses.¹³ In these experiments, a small amount of helium added to the system produced strong damping. Also, spreading of the damped wave packet was observed, a characteristic associated with Landau damping since high-frequency components are preferentially damped. At high helium-ion concentrations, the wave-packet velocity was observed to increase and the damping was observed to disappear. Based on a three-fluid model of the plasma, at high helium-ion concentration the wave-packet velocity is expected to increase toward that in a pure helium plasma. Since the ion wave velocity is then much greater than the thermal velocity of the helium ions, the damping is predicted to decrease.

The Landau damping caused by electrons in the plasma of pure xenon ions is quite small. The effect is calculated to be about 0.3 % of that caused by the helium in the data shown here.

Some final observations need to be mentioned. Since the wave energy decreases with distance as r^{-2} , our observations of received amplitude vary over a range of better than 10 to 1. Since the observed wave velocity and the damping factor are not functions of distance, the wave properties appear not to be amplitude dependent, and our simple, linear analysis probably is valid.

Thus, we have demonstrated in a simple fashion the Landau damping of ion-acoustic waves due to a trace of light ions in a plasma of heavy ions. Both the observed magnitude of the damp-

ing and the dependence of damping on frequency agree with a simple theory. The observed reduction of the damping with the increase of the ion-wave velocity is expected. The Landau damping can be turned on and off, or varied over a large range at will, without changing the other gross properties of the system.

*Research sponsored by the U. S. Atomic Energy Commission under contract with the Union Carbide Corporation.

†Consultant, University of Iowa, Iowa City, Iowa.

¹J. H. Malmberg and C. B. Wharton, *Phys. Rev. Letters* **13**, 184 (1964); J. H. Malmberg, C. B. Wharton, and W. E. Drummond, *Plasma Physics and Controlled Nuclear Fusion Research* (International Atomic Energy Agency, Vienna, 1966), Vol. 1, p. 485; J. H. Malmberg and C. B. Wharton, *Phys. Rev. Letters* **17**, 175 (1966); Gerard Van Hoven, *Phys. Rev. Letters* **17**, 169 (1966); H. Derfler and F. C. Simonen, *Phys. Rev. Letters* **17**, 172 (1966).

²A. Y. Wong, R. W. Motley, and N. D'Angelo, *Phys. Rev.* **133**, A436 (1964); A. J. Hopman, *Ned. Tijdschr.*

Natuurk. **31**, 266 (1965).

³A. Y. Wong, W. Hogan, and R. W. Motley, *Bull. Am. Phys. Soc.* **9**, 337 (1964).

⁴W. D. Jones and I. Alexeff, in *Proceedings of the Seventh International Conference on Ionization Phenomena in Gases*, edited by B. Perovic and D. Tosic (Gravdivinska Knjiga Publishing House, Beograd, 1966), Vol. 2, p. 330.

⁵I. Alexeff and W. D. Jones, *Phys. Rev. Letters* **15**, 286 (1965).

⁶W. D. Jones and I. Alexeff, *Bull. Am. Phys. Soc.* **12**, 770 (1967).

⁷I. Alexeff, W. D. Jones, and M. G. Payne, *Bull. Am. Phys. Soc.* **11**, 843 (1966).

⁸B. D. Fried and R. W. Gould, *Phys. Fluids* **4**, 139 (1961).

⁹R. W. Gould, *Phys. Rev.* **136**, A991 (1964).

¹⁰Obtained from NRC Equipment Corporation, 160 Charlemont St., Newton Highlands, Massachusetts 02161.

¹¹A. von Engel, *Ionized Gases* (Oxford University Press, London, 1965), 2nd ed., p. 63.

¹²Using a Waveform Eductor, Model TDH-9, made by Princeton Applied Research, Princeton, New Jersey.

¹³I. Alexeff, W. D. Jones, and D. Montgomery, *Bull. Am. Phys. Soc.* **12**, 770 (1967).

QUASIPARTICLE SELF-ENERGY AND SPECIFIC HEAT OF A FERMION LIQUID: APPLICATION TO He³†

D. J. Amit, J. W. Kane, and H. Wagner*

Laboratory of Atomic and Solid State Physics, Cornell University, Ithaca, New York

(Received 5 July 1967)

We have calculated the contribution, $\delta\Sigma(\vec{k}, \omega)$, of particle-hole excitations to the single-particle self-energy, $\Sigma(\vec{k}, \omega)$, of a Fermion liquid at zero temperature. Apart from regular terms we find that, for $0 \leq |\epsilon_q| \leq |\omega| \ll \omega_L \ll \mu$,

$$a_F(v_F k_F)^2 \delta \text{Re} \Sigma(\vec{q}, \omega) = [\phi_0 \omega^3 + \phi_1 \omega^2 \epsilon_q] \ln |\omega / \omega_L|. \quad (1)$$

$a_F^{-1} = 1 - \partial \Sigma(\vec{k}_F, \omega) / \partial \omega|_{\omega=0}$ is the renormalization constant, $v_F = k_F / m^*$ the Fermion velocity, m^* the effective mass, μ the chemical potential, and $\epsilon_q = v_F(|\vec{q}| - k_F)$. ω_L is a cutoff frequency which we shall discuss later. The dimensionless coefficients ϕ_i are obtained from Landau's theory of a Fermion liquid.¹ In general, every ϕ_i is the sum of contributions from incoherent spin² and density fluctuations, transverse excitations, and collective modes.³ The self-energy (1) yields a term $\sim T^3 \ln T$ in the specific heat C_V . In liquid He³ the dominant

contributions to C_V result from spin fluctuations.² Here we report on the salient features of the theory and on the results. Details will appear later.

Consider the vertex function,¹ $\Gamma_{\alpha\beta, \gamma\delta}(P; q, q')$, for the scattering of two particles, with four-momenta $(q, q' + P)$ and spins (α, β) , into a final state $(q + P, \gamma; q', \delta)$. The spectrum of particle-hole excitations is obtained from singularities (poles and branch cuts) in Γ in the energy-momentum transfer P . From the Pauli principle we find $\Gamma_{\alpha\beta, \gamma\delta}(P; q, q') = -\Gamma_{\alpha\beta, \delta\gamma} \times (q - q'; q' + P, q')$, so that singularities in P are identical to singularities in $q - q'$. For an isotropic system with spin-independent forces, $\Gamma_{\alpha\beta, \gamma\delta} = \frac{1}{2} \Gamma_1 \delta_{\alpha\gamma} \delta_{\beta\delta} + \frac{1}{2} \Gamma_2 \sigma_{\alpha\gamma} \sigma_{\beta\delta}$.

Ward identities¹ relate Γ to the Fermion self-energy, e.g.,

$$\frac{\partial \Sigma(q)}{\partial q_0} = - \int \frac{d^4 q'}{(2\pi)^4} \Gamma_1^\omega(q, q') (G^2)_{q'}^\omega, \quad (2)$$

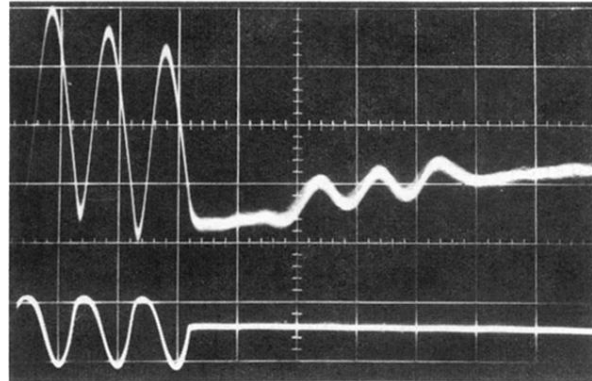


FIG. 2. Typical transmitted and received signals over short distances without using coherent detector. Lower trace, transmitted signal. Upper trace, received signal. Note the strong, directly coupled signal on the receiver trace which is separated from the weaker, ion-wave signal by time of flight. Vertical axis, amplitude (relative units). Horizontal axis, time ($10 \mu\text{sec}/\text{large division}$). The gas used is xenon.